5-15-1953

A beta-ray spectrometer for coincidence measurements

R. T. Nichols
Iowa State College

A. V. Pohm
Iowa State College

J. H. Talboy Jr.
Iowa State College

E. N. Jensen
Iowa State College

A beta-ray spectrometer for coincidence measurements

Abstract
An intermediate image beta-ray spectrometer has been constructed utilizing the focusing properties of a U-shaped magnetic field distribution. The construction and performance of the instrument are discussed. A transmission of ten percent has been attained with a resolution of about six percent. A scintillation spectrometer is used in conjunction with the intermediate image spectrometer for the purpose of making coincidence measurements.

Keywords
Ames Laboratory

Disciplines
Engineering | Physics

ISC-345

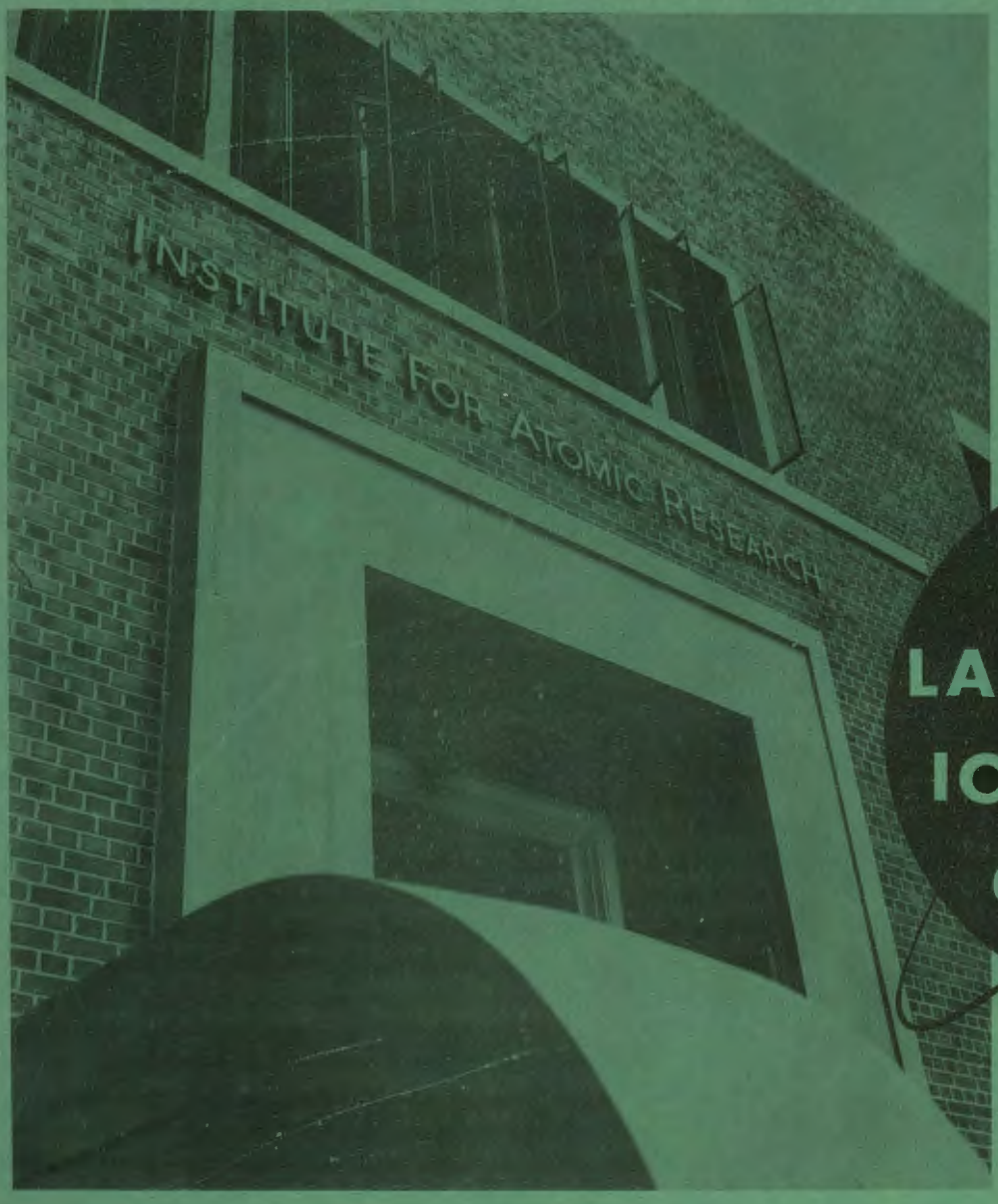

AMES LABORATORY IOWA STATE COLLEGE

A BETA-RAY SPECTROMETER FOR COINCIDENCE MEASUREMENTS

ISC-345

UNITED STATES ATOMIC ENERGY COMMISSION

A BETA-RAY SPECTROMETER FOR COINCIDENCE MEASUREMENTS

by

R. T. Nichols, A. V. Pohm, J. H. Talboy, Jr., and E. N. Jensen

May 15, 1953

Ames Laboratory
at
Iowa State College
F. H. Spedding, Director
Contract W-7405 eng-82

This report is distributed according to the category Instrumentation as listed in TID-4500, April 15, 1953.

A BETA-RAY SPECTROMETER FOR COINCIDENCE MEASUREMENTS

R. T. Nichols, A. V. Pohm, J. H. Talboy, Jr., and E. N. Jensen

ABSTRACT

An intermediate image beta-ray spectrometer has been constructed utilizing the focusing properties of a U-shaped magnetic field distribution. The construction and performance of the instrument are discussed. A transmission of ten percent has been attained with a resolution of about six percent. A scintillation spectrometer is used in conjunction with the intermediate image spectrometer for the purpose of making coincidence measurements.

I. INTRODUCTION

In pursuing a particular problem in beta-ray spectroscopy, a spectrometer is desired which has not only the necessary energy resolution but also sufficient luminosity (source area times transmission) to minimize statistical questions. In order to make coincidence measurements with reasonable precision, it is necessary to have a beta-ray spectrometer of high luminosity and moderate energy resolution. The intermediate image beta-ray spectrometer, which utilizes the focusing properties of a U-shaped field,[1] satisfies these requirements. This paper presents some details on the design and operation of such an instrument.

II. DESIGN OF THE SPECTROMETER

A. Intermediate Image Focusing

The availability of short-lived, low activity samples of radioisotopes from the Iowa State College synchrotron and the need for high counting rates for coincidence spectra prompted the planning of a spectrometer of high luminosity. An iron-free thin-lens spectrometer[2] had previously been constructed. After a modification in the baffle system to utilize ring focusing,[3] a transmission of about 0.3 percent is obtained with a resolution of approximately four percent.

Spherical aberration limits the usable solid angle in most beta-ray spectrometers. This aberration is least for electron paths which follow close to some line or surface which may be termed the optical axis of the system. If a set of baffles is arranged so as to accept only these central or paraxial rays, the spherical aberration will be minimized. However, in the ordinary magnetic lens

spectrometer these central rays cannot be used because the optical axis is the straight line between the source and the counter and there is no energy dispersion in this region. Also, gamma-rays, which in this case may follow the optical axis, must be prevented from reaching the detecting apparatus. Therefore, electrons are used which come off the source at some small angle relative to the axis. There is greater energy dispersion for greater angles of emission relative to the axis but there is also an increase in spherical aberration which makes it unprofitable to use larger angles.

Glaser[4] has calculated a field form for zero spherical aberration as shown in Fig. 1. Though the infinite field intensity at the ends cannot be achieved, it can be shown[5] that a decrease in spherical aberration might be expected if the field along the axis is U-shaped with finite values at the ends.

Siegbahn and Slätis[1,5] have built several spectrometers to investigate the possibilities of the U-shaped field. As a result, intermediate image focusing was first realized experimentally. With the proper high gradient U-shaped field, the most valuable portion of the radiation beam may be utilized. The outer edge of the beam as it passes the central plane will contain the paraxial rays of minimum spherical aberration. A ring aperature may be placed in the central plane to transmit only the outer portion of the beam. Good energy resolution will be obtained in this way due to high energy dispersion and low spherical aberration. At the same time the transmission is greatly enhanced by a ring focus in this plane.

A schematic, axial cross section of the spectrometer which Slätis and Siegbahn[1] used in achieving intermediate image focusing is shown in Fig. 2. The spectrometer has a magnetic iron yoke with pole pieces to aid in forming a U-shaped field. By increasing the currents in the outer pair of coils relative to the currents in the other three, the gradient may be increased. As this ratio of currents was increased to a particular high value, a sharp increase in transmission occurred. As the gradient was further increased the transmission reached a maximum value and rapidly diminished. Further examination brought to light the focusing principle which caused this increase.

The trajectories of monoenergetic electrons having various angles of emergence from the source were found by Slätis and Siegbahn[1] to be somewhat as shown in Fig. 3. At a particular angle of emergence relative to the axis of symmetry (depending upon the gradient of the field) the electron trajectories are symmetric to the midplane of the spectrometer. Electrons which leave the source at a greater angle relative to the axis have trajectories which are bent more as they travel farther in the more intense field at the end of the spectrometer. If the slope of the U-shaped field is great enough, they are curved sufficiently to cross the trajectories of the symmetric rays before they reach the central plane. If the gradient is not too great, the straighter paths of the

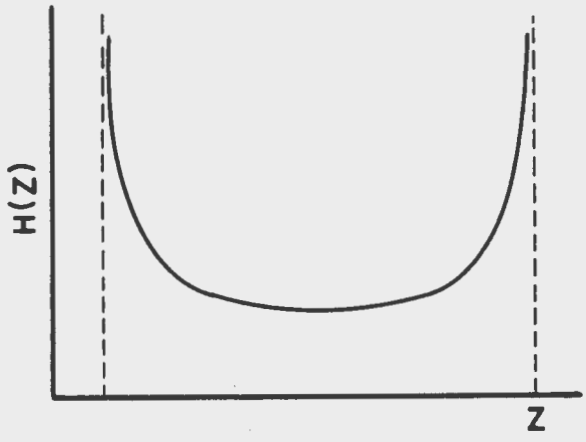

Fig. 1 - Magnetic field form for zero spherical aberration as calculated by W. Glaser.

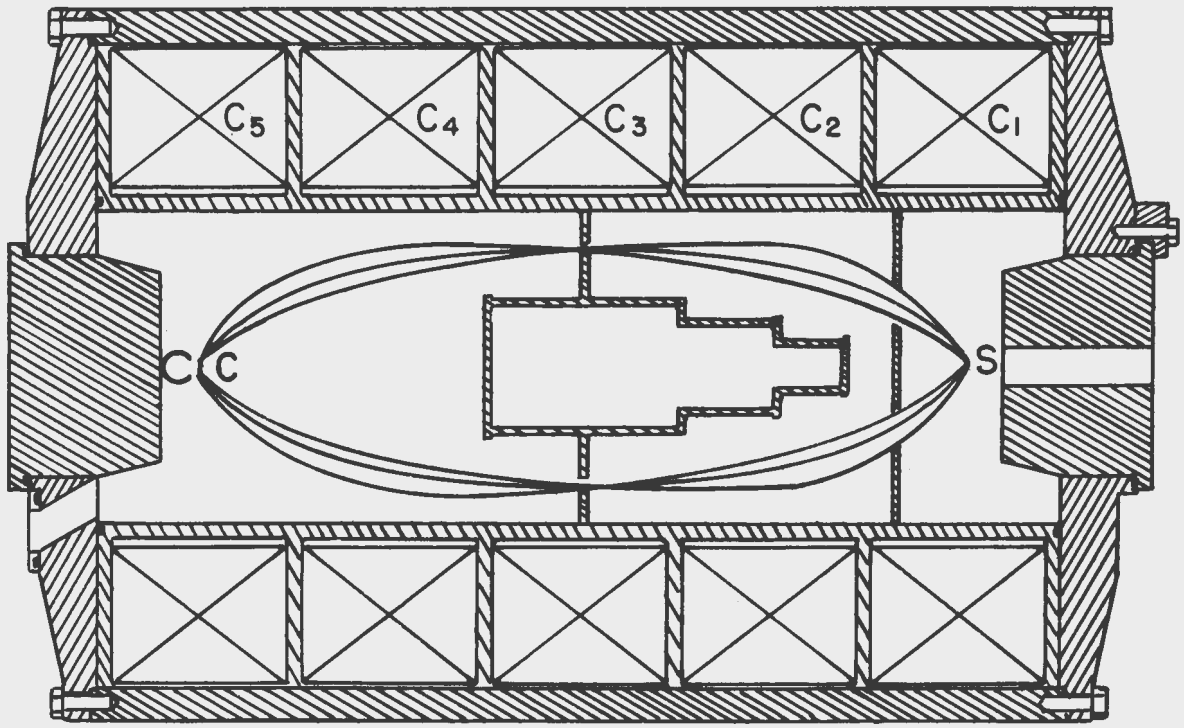

Fig. 2 - Schematic axial cross section of the intermediate image beta-ray spectrometer of Slätis and Siegbahn.

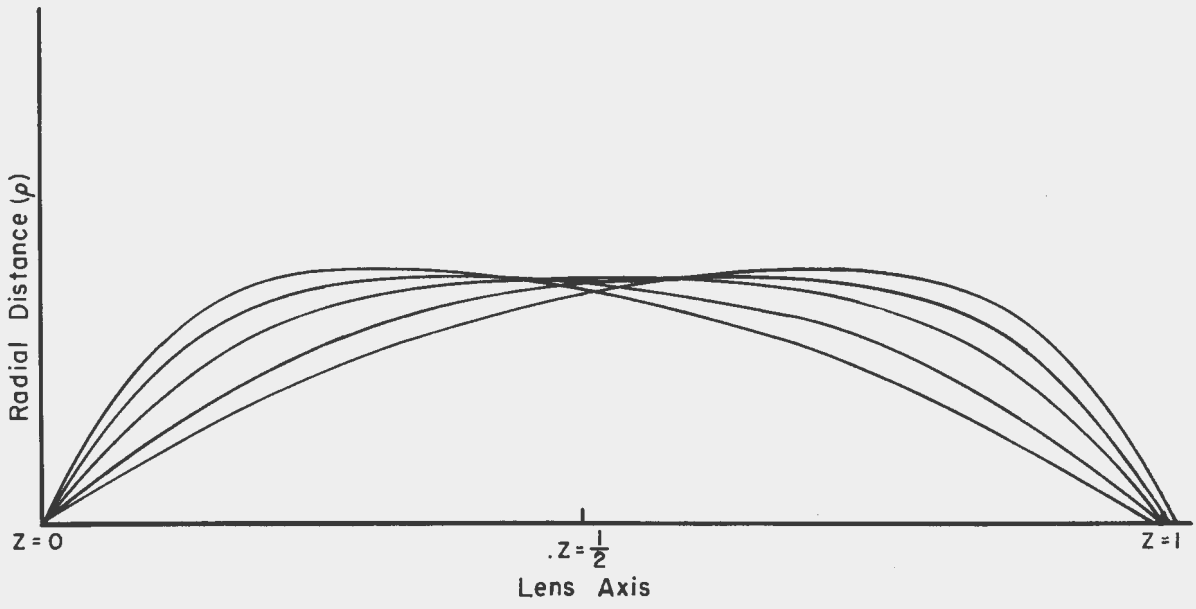

Fig. 3 - Trajectories of monoenergetic electrons in an intermediate image beta-ray spectrometer.

electrons coming off the source at smaller azimuthal angles do not cross the trajectories of the symmetric rays until after they reach the midplane. Thus there is a sharp edge at the midplane outside of which no electrons of this energy can pass. This is analogous to the well known sharp edge in semicircular focusing. Inside the sharp edge the intensity gradually diminishes toward the axis. No doubt, the rate of this decrease of intensity is considerably influenced by the particular form of the U-shaped field by which the intermediate image is achieved. The trajectories of electrons from a point source which pass the central plane near the outer edge of the beam meet again in a point focus on the axis at the other end of the spectrometer. Thus a ring aperature in the central plane may be constructed to transmit these rays of particularly low spherical aberration while eliminating the non-paraxial rays which would contribute to a loss in resolving power. The low spherical aberration makes it practical to use a relatively large aperature width when high transmission is demanded. Slätis and Siegbahn[1] reported the attainment of eight percent transmission with a resolution of about four percent. The point focus at the end permits the use of a small detection area and results in a low count of scattered radiation.

Richardson[6] has published a theoretical investigation dealing with the magnetic focusing properties of the field obtained between two hyperbolic pole surfaces. He found that an intermediate ring image such as this is formed by electrons which leave one pole at an angle of nearly ninety degrees relative to the axis. However, there may be some practical difficulties in source mounting and detection in a spectrometer of this type. Bothe[7] has given a treatment of the focusing properties of a U-shaped field formed by two thin magnetic lenses. Two such lenses can be arranged to form an intermediate image in the symmetry plane. However, the spherical aberration is greater in this case than with the field shape used by Slätis and Siegbahn.

B. Details of Construction

The intermediate image type of spectrometer appeared to be well suited for high transmission. It has the added advantage of simple construction and maintenance. The magnetic yoke aids in forming the U-shaped field and also decreases the magnetic reluctance. Moreover, it shields the spectrometer from external fields and insures that the focusing will be axially symmetric. The disadvantage of possible non-linearity in the current-field relation due to the presence of iron did not appear to be great. Slätis and Siegbahn[1] found that the departure from linearity was less than $\pm$ 1% from 0.25 amp to 10 amp when the lens was demagnetized. This corresponds to an energy range of 3 kev to 1.8 Mev. Furthermore, a calibration curve may be obtained to determine the actual current-momentum relationship.

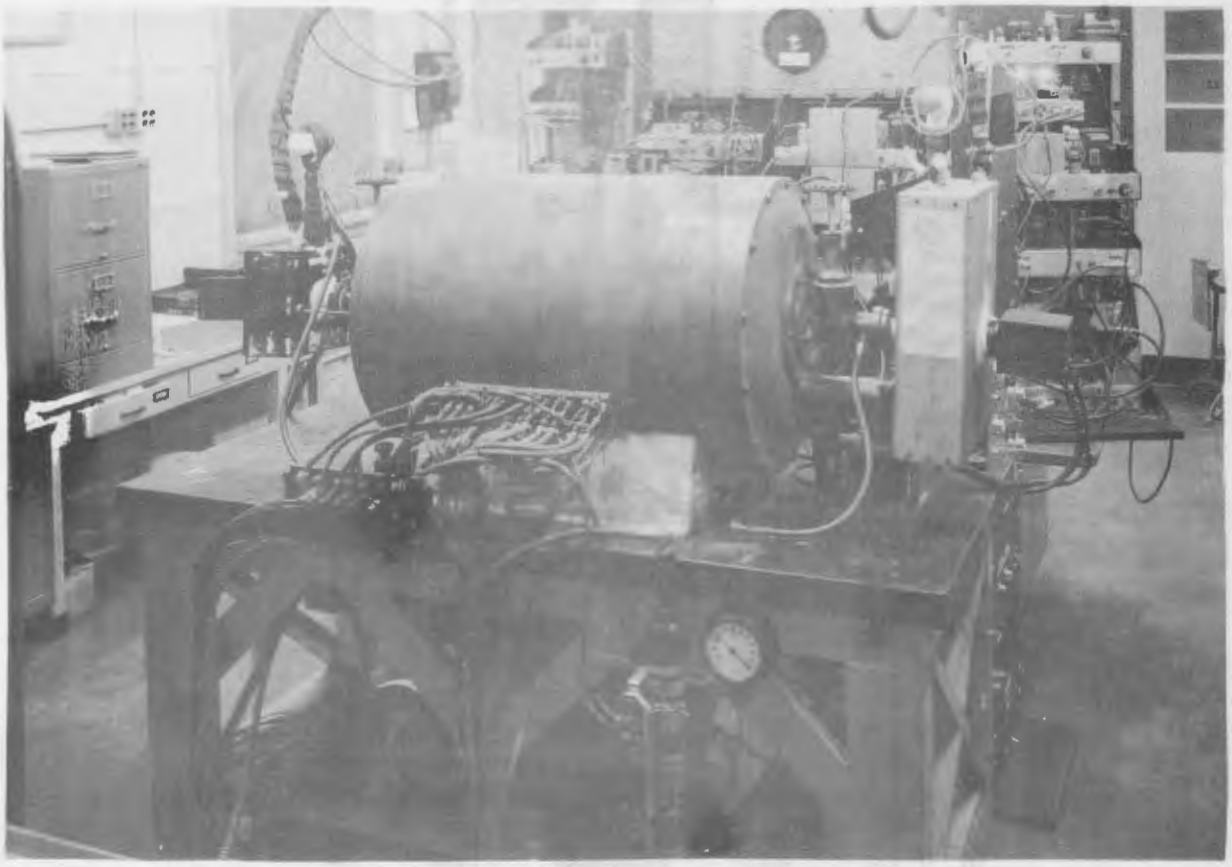

Fig. 4 - Photograph of the spectrometer.

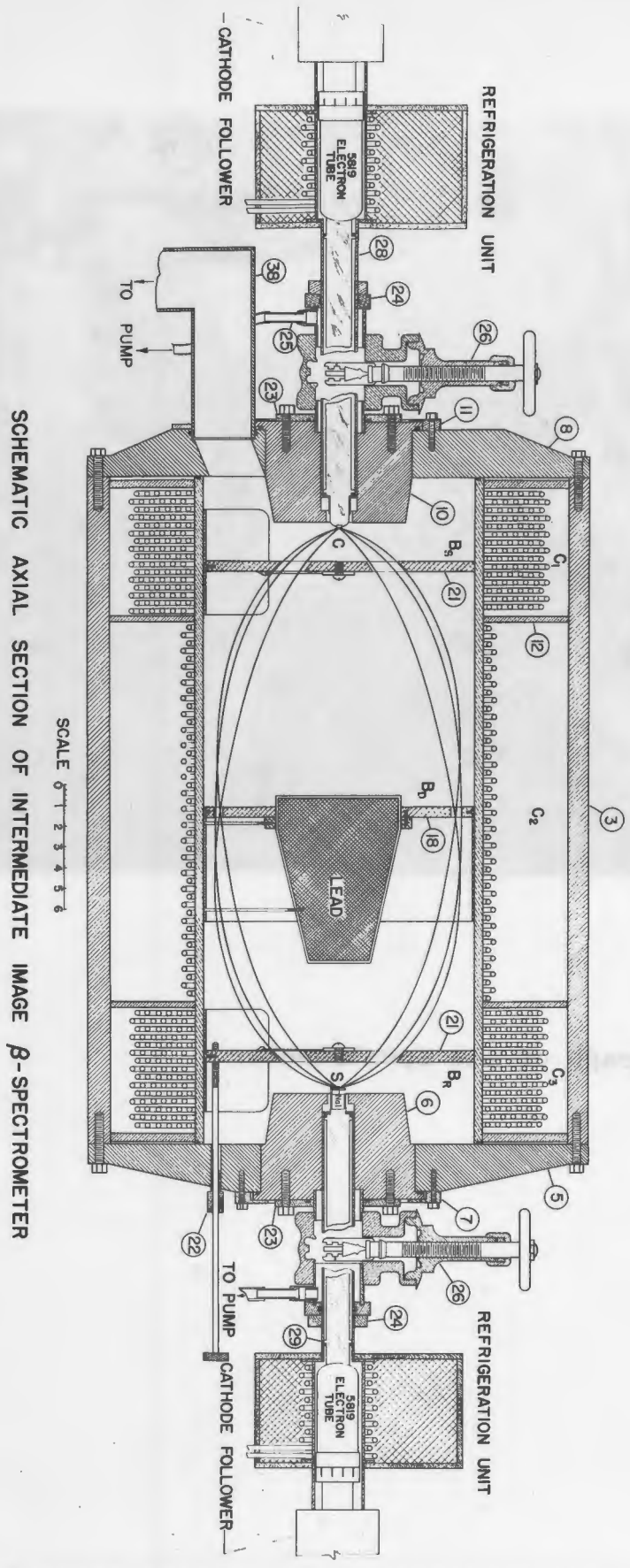

Fig. 5 - Axial cross section of the spectrometer.

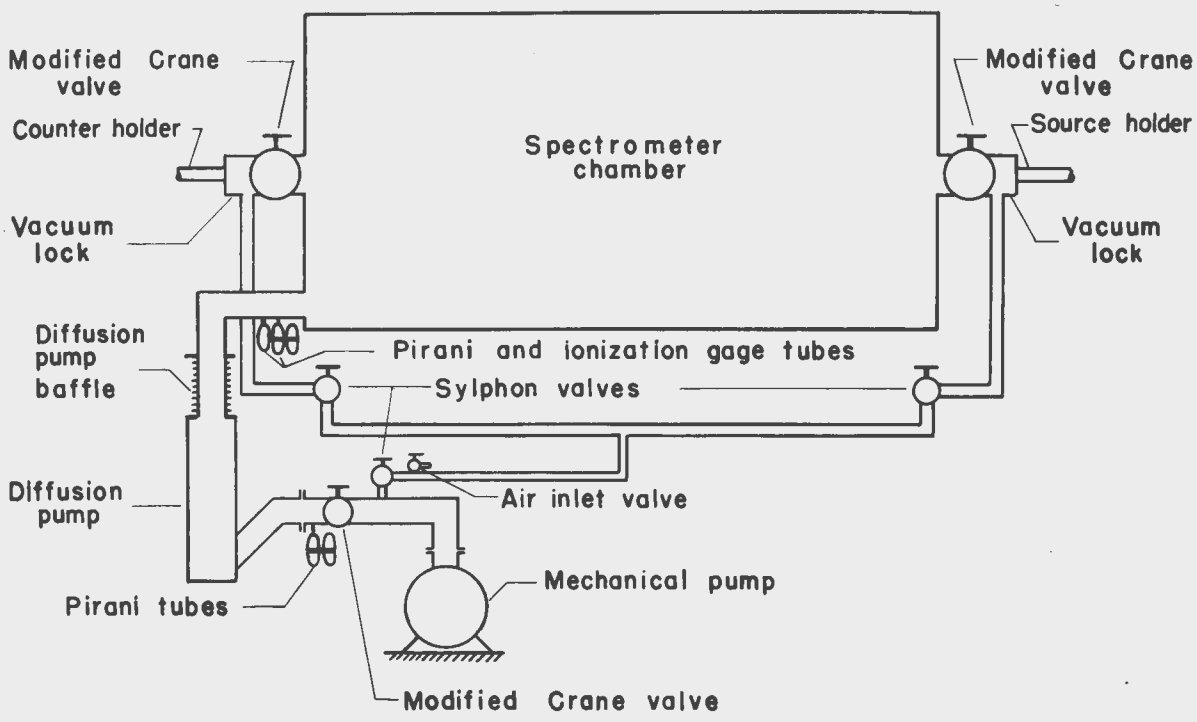

Fig. 6 - Schematic view of the vacuum system.

The practical area for sources increases as the square of the linear dimensions of the spectrometer. Therefore, higher luminosity is obtained if the instrument is made large. The size was limited by considerations such as the machining and handling of parts.

Considerable time and preliminary experimentation were eliminated by making the spectrometer dimensions somewhat proportional to those in the spectrometer of Slätis and Siegbahn.[1] It was then possible to estimate from their results the number of ampere-turns necessary for the desired energy range. This information was used to calculate the power demands of the spectrometer and the heat to be removed by the cooling system.

The completed spectrometer is pictured in Fig. 4. A schematic axial cross section is shown in Fig. 5. A discussion of the construction follows.

(1) The Vacuum System. The spectrometer chamber is evacuated by means of an oil diffusion pump (capacity - 275 liters/sec at 10^{-4} mm.) backed by a Welch duo-seal mechanical pump. Fig. 6 shows, schematically, the principal parts of the vacuum system. The vacuum line enters the spectrometer chamber through an opening in the end plate at the counter end. The vacuum chamber is formed by the brass cylinder of the coil spool and the ends of the iron yoke. The end plates are sealed against the ends of the brass cylinder by means of square rubber gaskets. All other seals are made with O-rings. Sources or counters may be inserted or removed from the spectrometer through vacuum locks on either end. With this system a pressure of less than 5×10^{-5} mm Hg is normally maintained in the spectrometer.

(2) The Magnetic Yoke. The magnetic yoke is made of Armco magnetic iron. The cylindrical shell surrounding the coils is 32.25 inches long, 25 inches o.d. and one inch thick. The end plates bolt on the ends of the cylindrical shell and seat against the vacuum gaskets at the ends of the brass cylinder. They are one inch thick on the periphery and 2.25 inches thick on the inner edge. The pole shoes slip into the end plates and are sealed by O-rings. Since the poles extend 2.125 inches into the spectrometer, the inner pole faces are 28 inches apart.

(3) The Coils and the Cooling System. The coils are wound in three sections as shown in Fig. 5. The coil spool is brass with the spacing of the three coil sections being 6.1, 18.3, and 6.1 inches, respectively. Each section is lined with a double layer of silicone-varnished glass fabric, 0.01 inch thick. The coils are wound with three-sixteenth inch o.d. copper tubing which has a 0.035 inch wall and is covered with a double layer of Silotex insulation. A layer of the glass fabric is wrapped between each layer of tubing. The coil was impregnated with a silicone insulating varnish, prebaked at a temperature of about 170°F for 48 hours,

and baked at a temperature of about 300°F for 12 hours. The coils, C_1 and C_3, each contain 577 turns of copper tubing; C_2 contains 180 turns.

The terminals of the copper windings pass through a slot in the iron cylinder to a terminal board on the side of the spectrometer. There are twelve pairs of terminals forming twelve parallel paths of approximately equal length through which distilled water is pumped to carry off the heat generated in the coils. The heated water is passed through a heat exchanger where the heat is transferred to tap water which is discharged. The cooled, distilled water is then re-cycled through the coils.

A water-cooled shunt resistance of brass wire is connected across the center coil and adjusted to give the optimum field shape with the coils in series, electrically. The heated water from the coils passes over the shunt resistance and thus has a temperature variation of twice the average temperature variation in the copper coils. The temperature coefficient of resistance for brass is about one half of copper, thus the resistance of the parallel circuit elements will change proportionally.

(4) The Baffle System. The spectrometer baffle system is shown in the cross-sectional view (Fig. 5). The baffles are aluminum and are one half inch thick. The defining baffle, B_D, forms a ring aperature with an outside diameter of twelve inches. The width of this aperature may be varied by inserting center shutters of various diameters. The resolving baffle, B_R, is positioned externally by means of a pair of rods extending through the end plates. The central shutter of the resolving baffle may be changed to various sizes associated with the various shutters used in the defining baffle. The scattering baffle, B_S, has an opening which corresponds to the widest defining aperature width and is left fixed. There is a layer of magnesium 1/16 inch thick covering the surface of the brass cylinder between the defining baffle and the scattering baffle. The lead plug is 8 inches long and is covered with a layer of aluminum 1/16 inch thick.

(5) Source Mountings. The sources are mounted in the spectrometer as indicated in Fig. 7. Beta sources or internally converted gamma sources are deposited on a Formvar-polystyrene film which is mounted on a Lucite holder. Photo conversion gamma sources are deposited in the cavity of a brass holder as shown. The radiator foil is attached to a copper cap which absorbs the electrons emitted by the source.

(6) The Current Servo. A 25 kilowatt motor-generator provides the current for the spectrometer coils. The current is set by varying the field current of the generator with a current control device. The current control contains a servo-mechanism by which the current may be kept at a setting well within one part in a thousand. The current is controlled from 1/2 to 100 amperes.

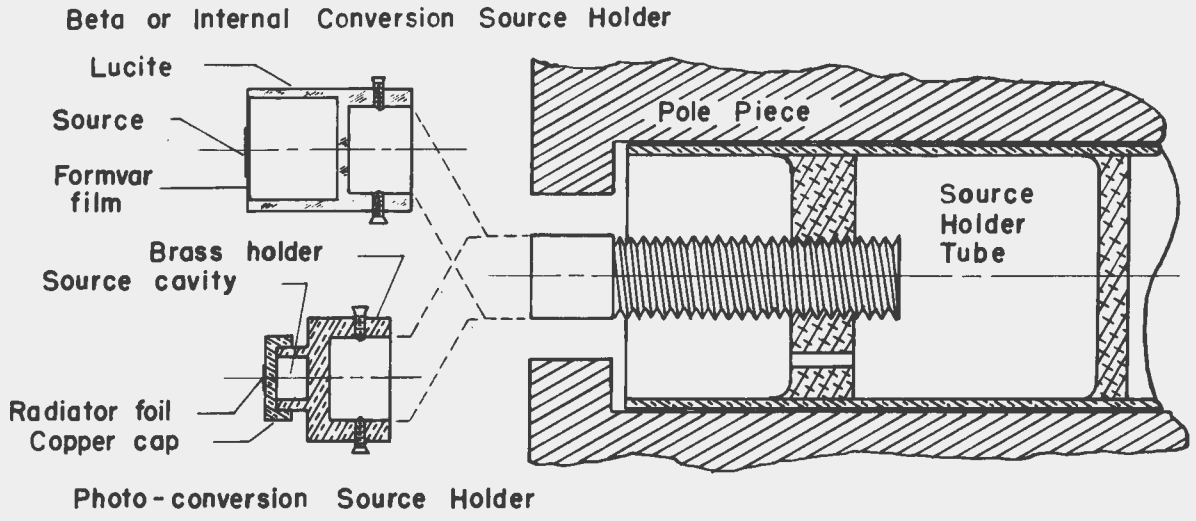

Fig. 7 - Source holders and positioning in spectrometer.

(7) Counters and Associated Electrical Circuits. The beta-particle detector is an anthracene crystal which is 3/32 inch thick and 5/8 inch in diameter. It is mounted on the end of a Lucite light pipe by means of small spring clips as shown in Fig. 8. The optical contact between the anthracene and the Lucite is made with a silicone oil. The photons created in the crystal by the incident beta-radiation are transmitted by means of the light pipe to a 5819 photomultiplier tube outside the iron yoke.

Fig. 9 shows the arrangement used on the source end of the spectrometer for coincidence measurements. The source material is deposited on a Formvar-polystyrene film which is supported by an aluminum ring. A sodium iodide crystal 3/4 inch thick and 7/8 inch in diameter is used as the gamma-ray detector. It is preserved by the layers of MgO and $Mg(ClO_4)_2$. Optical contact between the crystal and the light pipe is made with the silicone oil. An aluminum absorber of the necessary thickness is placed between the source and the sodium iodide crystal to prevent beta-particles from reaching the crystal.

The electrical circuits associated with the counting apparatus are indicated in Fig. 10. The pulse-height analyzer determines the energy of the gamma-rays that are counted by the gamma-scaler. The spectrometer setting determines the energy of the beta-particles that are counted by the beta-scaler. The beta-channel and the gamma-channel may be operated in conjunction with the coincidence circuit to measure the coincidences between radiation particles, or they may be operated independently as the beta-ray spectrometer counter and as a scintillation spectrometer, respectively.

The pulse shaping in the gamma-channel is done to give more repeatable and accurate results when using the pulse height analyzer. The pulses from the photomultiplier tube, produced by mono-energetic gamma-rays, contain approximately the same total charge though they vary in voltage amplitude and in duration. The pulses are of short duration so an RC integrating circuit is used which measures the total charge of the pulse. The discharge time of the RC circuit is about 50 microseconds. The output of the integrating circuit is fed into the pulse shaper which consists primarily of a stage of amplification which a shorted delay line in the plate circuit. The input signal has a sharp rise with a gradual decline caused by the RC circuit's slow discharge. The signal is then squared by the shorted delay line which reflects an inverted signal which is delayed about one half microsecond. The resulting square pulse is about one half microsecond wide with an amplitude proportional to the energy of the original gamma-ray.

The amplifiers used in both channels have an even gain characteristic from about 50 cycles up to 15 megacycles. The amplifiers consist essentially of three RC coupled stages using 6AG7 amplifier tubes with 2200 ohm plate load resistors. The beta-amplifier has an additional stage of amplification and a signal limiting stage.

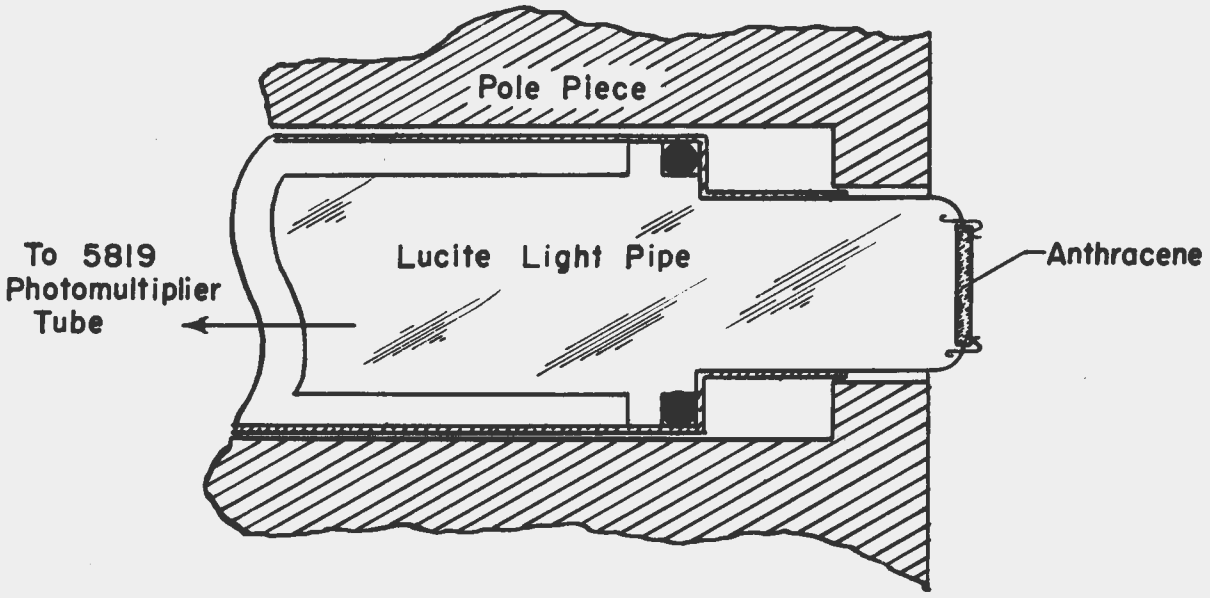

Fig. 8 - Anthracene crystal and Lucite pipe for beta-ray counter.

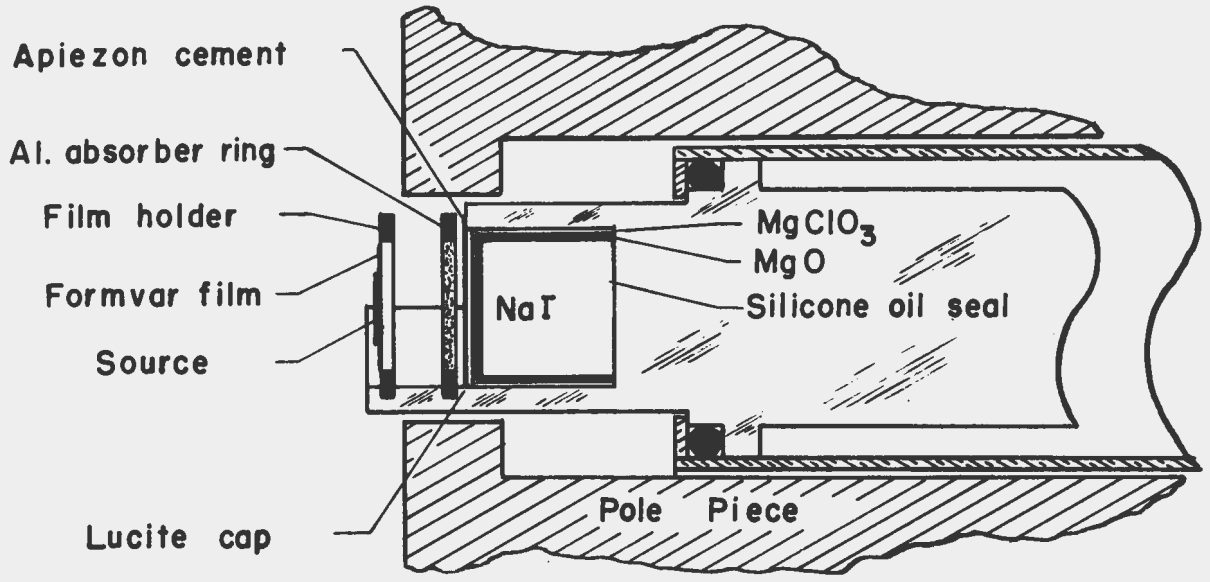

Fig. 9 - Arrangement of source and crystal of gamma-ray counter for coincidence measurements.

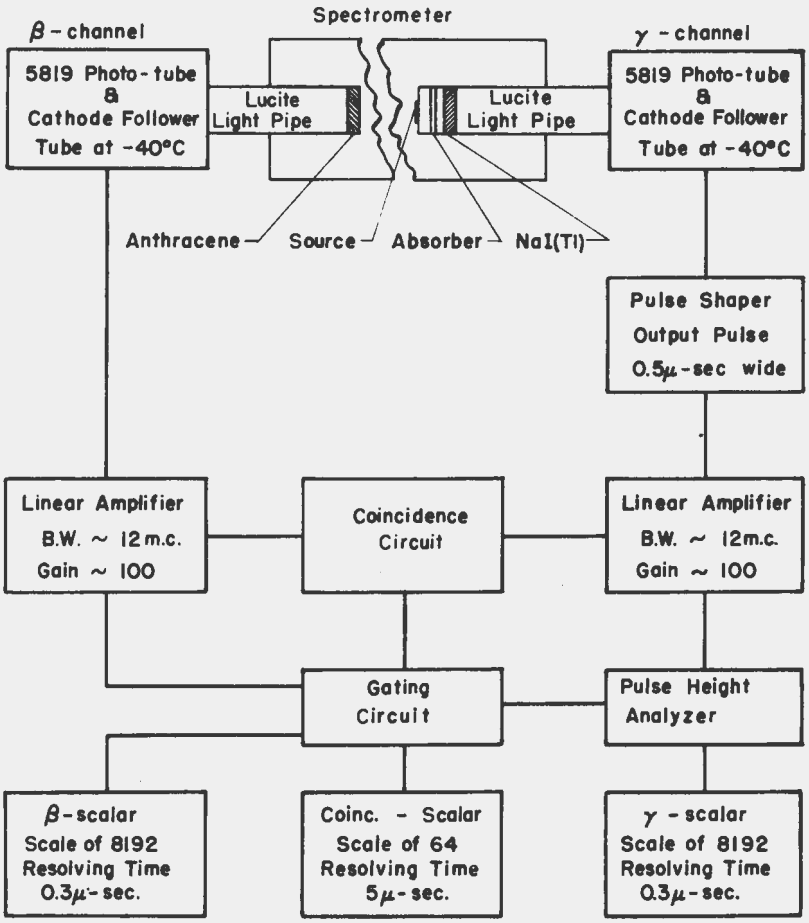

Fig. 10 - Block diagram of counting circuits.

Pulses from the linear amplifiers are fed into the coincidence circuit. A 6BN6 gated-beam tube operates as a fast coincidence circuit[8] with a possible resolving time of less than 10^{-9} seconds. Since the pulses are of longer duration, it is the pulse duration that determines the effective resolving time. The length of a pulse from the beta-channel is influenced by the energy of the initiating beta-particle so the resolving time is dependent upon the beta-ray energies. Another effect which influences the effective resolving time will be mentioned in the next section.

The pulse height analyzer is of the type developed by Francis, Bell, and Gundlach.[9] It consists primarily of two biased amplifier circuits and an anticoincident circuit. The first biased amplifier circuit passes a signal only if that signal is greater than some value which is determined by a variable bias setting. If the remaining part of the signal coming from the first biased amplifier exceeds the bias of the second biased amplifier, it will pass to the anticoincidence circuit and no signal will be transmitted. However, if the signal is large enough to trigger the first amplifier and not the second, a pulse will be transmitted from the anticoincidence tube. Thus by adjusting the first bias the lower limit of accepted pulse height is determined and by adjusting the second bias the acceptance increment is selected.

There are usually after-pulses following a signal from one of the phototubes. The number and amplitude of these after-pulses are functions of the energy of the gamma-rays or beta-particles initiating the signal. A gating circuit is used to reduce the number of possible coincidences to one for each pair of beta and gamma signals. The gating circuit consists, essentially, of three single-kick multivibrators and two 6BN6 gating tubes. Each multivibrator produces a square wave 10 microseconds long. Signals from the beta-amplifier are fed into one multivibrator and signals from the coincidence circuit are fed into another. The square wave pulses from these two multivibrators are put on the two control grids of the first gating tube so that a square wave is produced for the period of coincidence between the two waves. This square wave is put on one control grid of the second gating tube while the other grid is operated by the pulses from the third multivibrator which is triggered by signals from the pulse height analyzer. The result is that only coincidences between beta-rays and gamma-rays of the selected energies are counted and no extra coincidences from after-pulses. The resulting dead time is 10 microseconds for each coincidence pulse.

Beta-ray and gamma-ray signals could be taken from the beta-amplifier and the pulse height analyzer and used to trigger single-kick multivibrators and the resulting square waves differentiated to eliminate after-pulses. However, the variable delay from the pulse height analyzer would prevent use of these signals in the coincidence circuit. Therefore, the coincidence circuit is operated by the signals from the beta- and gamma-amplifiers and the gating

circuit used to eliminate the coincidences from after-pulses and from gamma-rays of other than the desired energy.

The beta-scaler and the gamma-scaler are of a binary type having a resolving time of 0.3 microsecond [10] and capable of counting more than 1,000,000 counts per minute. Each consists of thirteen binary stages followed by a mechanical register. The coincidence scaler is a standard model using a binary scale of 64. It has a five microsecond resolving time. The beta-scaler is operated by pulses from the multivibrator in the gating circuit which is triggered by beta-signals. This eliminates the counting of after-pulses and results in a dead time of 10 microseconds per counted beta. The gamma-scaler takes signals from the univibrator which is triggered by the pulse height analyzer although the after pulses have already been eliminated by the pulse-height analyzer.

III. ADJUSTMENTS AND PERFORMANCE MEASUREMENTS

The spectrometer coils were connected in series, electrically, and the magnetic field intensity measured along the spectrometer axis. A plot of the field distribution with a current of 1.5 amp in the coils is shown in Fig. 12.

The central defining baffle primarily determines the transmission and resolution of the spectrometer. The source and counter positioning and the field shape adjustments were determined with the central baffle having a slit width of 3/8 inch and with no other baffle in the spectrometer. The conversion line from the decay of Cs^{137} was used to compare the relative transmissions as the various adjustments were made. Shunt resistances were connected across the center coil or across the end coils to vary the gradient of the field. This was repeated for various source or counter positions until the conditions for maximum transmission were determined.

Fig. 13 shows the relative transmission as a function of the ratio of ampere-turns in the center coil to the total number in the three coils. Though the transmission peak is relatively sharp in this plot, the value of the shunt resistance is not critical since the turns ratio in the coils is already near the desired ampere-turns ratio for optimum operating conditions. The final arrangement of coil connections for optimum transmission uses 346 turns in each end coil, 180 turns in the center section and no shunt resistance. A low-energy range was formed using 113 turns in each end coil, 90 turns in the center coil and a shunt resistance of 0.365 ohm across the center section. This shunts about 34 per cent of the current around the center coil.

Fig. 14 shows the effect on the relative transmission and half-width when the source is moved relative to the counter. The source position was varied with the counter window placed 3/8 inch from the pole face. A deviation of 1/32 inch from the position of maximum

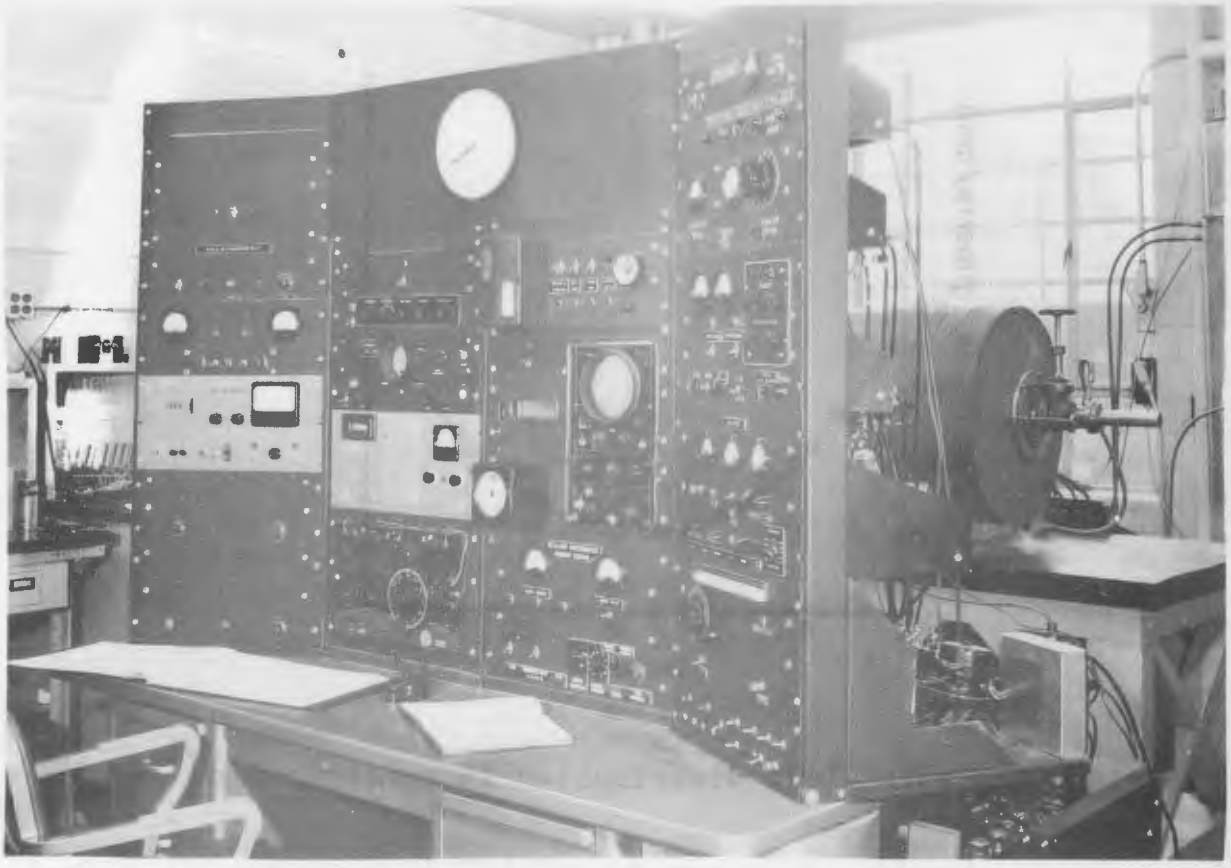

Fig. 11 - Photograph of the spectrometer control panel.

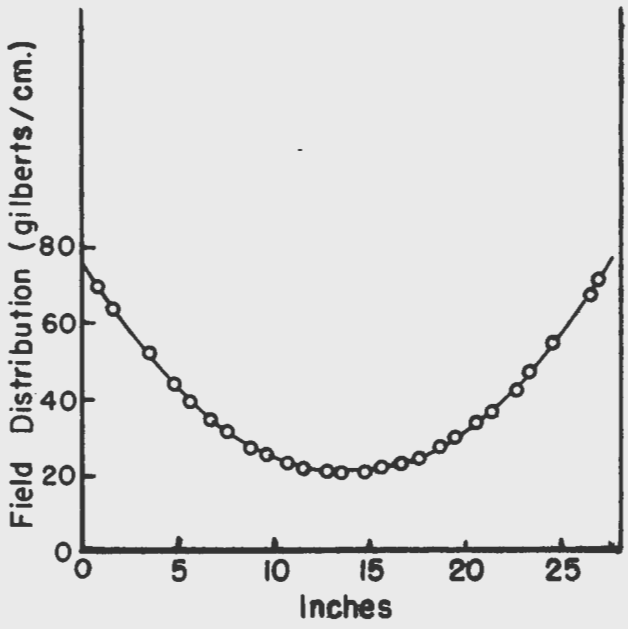

Fig. 12 - Magnetic field distribution in spectrometer.

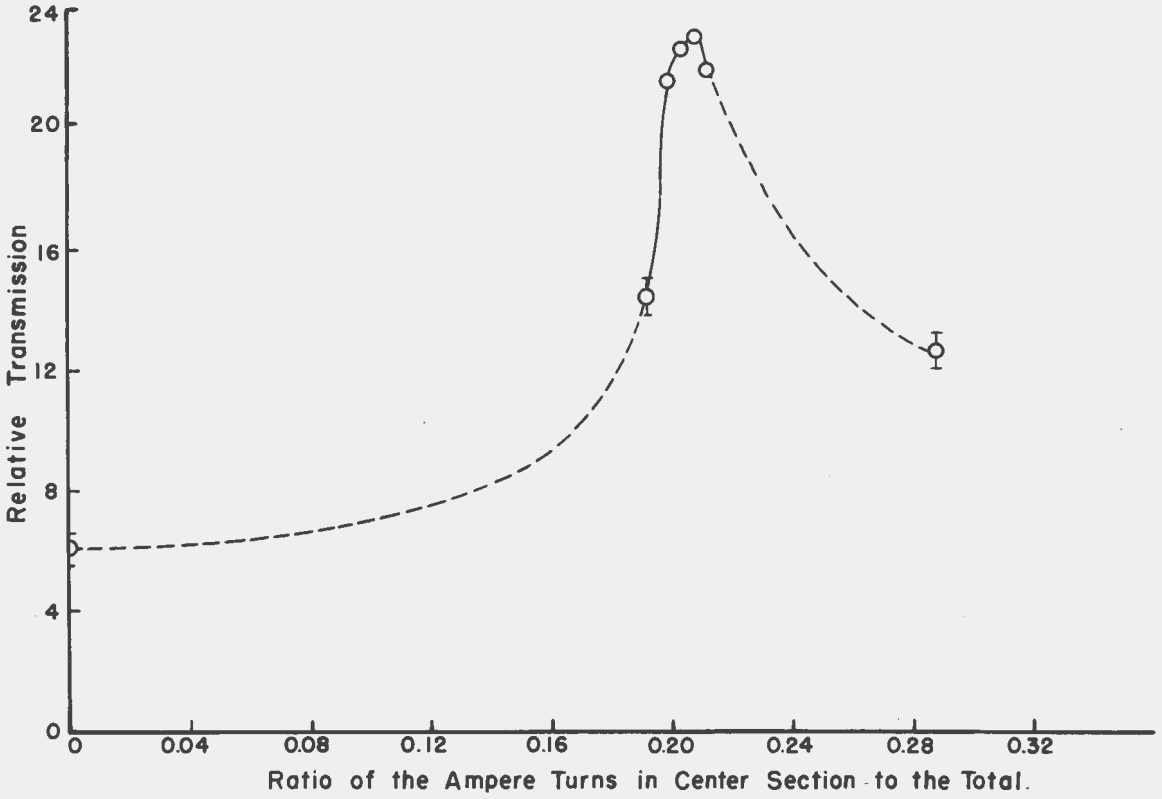

Fig. 13 - Relative transmission versus the ratio of ampere-turns in the three coils.

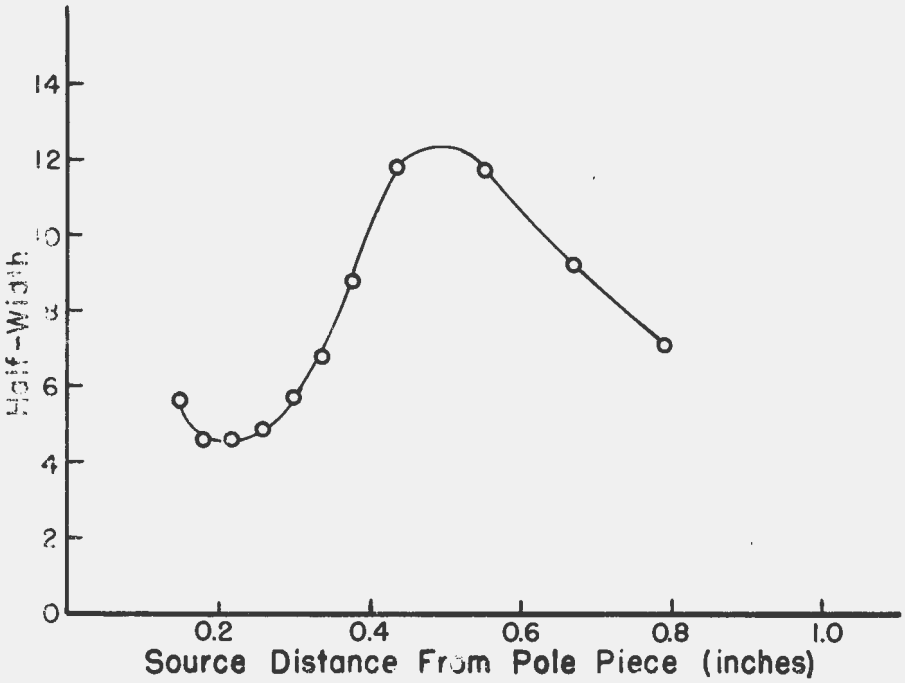

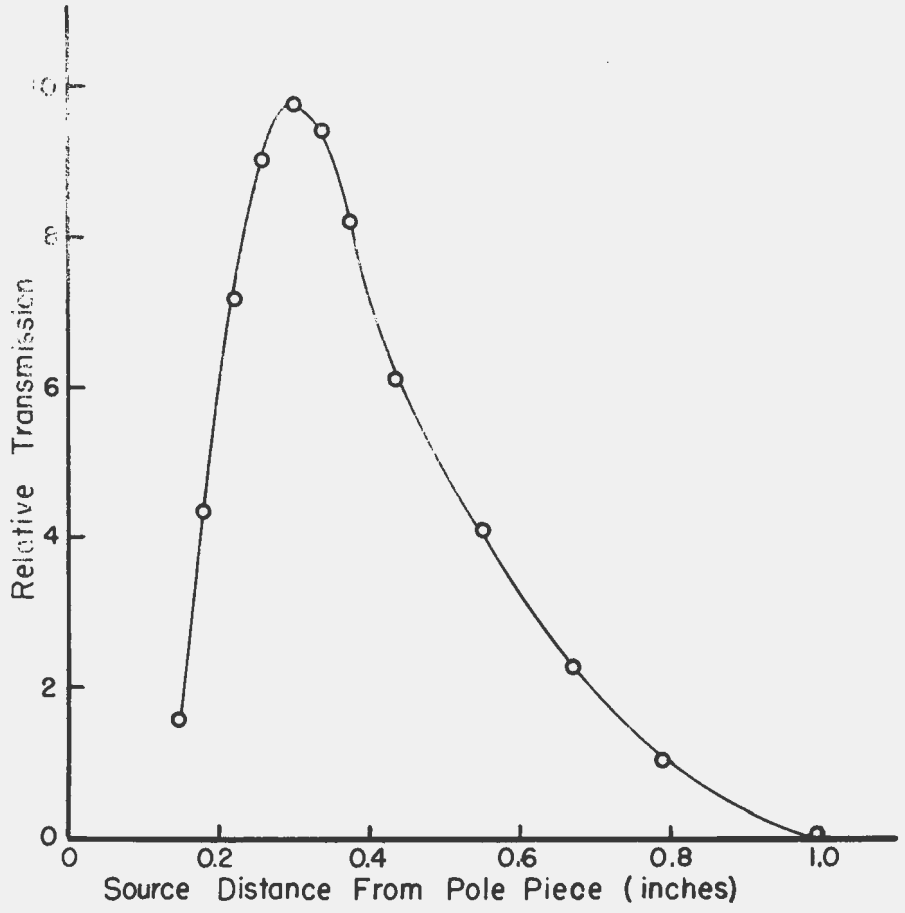

Fig. 14 - Transmission and half-width as a function of source position (with counter position fixed).

transmission resulted in a two or three per cent decrease in transmitted intensity. A deviation of 1/16 inch caused the intensity to drop more than ten per cent. The half-width is near the minimum at the point of highest transmission so the maximum transmission is obtained with little sacrifice of resolving power. When the source and counter were placed progressively closer to the pole faces (shifting the source for optimum transmission with each counter placement) the resolution remained approximately constant while the transmission slowly increased. The source and counter are positioned 5/32 inch and 3/16 inch, respectively, from the pole faces in order to avoid excessive scattering.

The results of various defining baffle slit widths are shown in Fig. 15. The source used was approximately 0.8 cm in diameter. The effect of the resolving baffle (see Fig. 16) is a marked increase in resolution with little change in transmission. The trailing edge of the gamma line is reduced and the resulting line shape is almost symmetrical.

Geiger counters were used as the beta-detectors in the adjustments previously discussed. Fig. 17 indicates the geometry of the counter. The counter window was of Formvar with a thickness of approximately 300 $\mu g/cm^2$. Photographs revealed that the focusing image was about 1/2 inch in diameter at the counter and that the angle of approach of the electrons was about 49° relative to the axis. Fig. 18a shows a Kurie plot of Y^{90} from spectrometer data obtained with a Geiger counter before the scattering baffle was inserted. Y^{90} is known to be a first-forbidden transition with a spin change of two and a parity change. It has been shown to yield a linear Kurie plot[11] when the "a" correction factor is used. A scintillation counter produced a greatly improved Kurie plot (Fig. 18b) so the defects of the first Kurie plot may not be attributed entirely to scattering in the spectrometer. It had been noticed that the counting rate was a sensitive function of the distance of the anode bead from the counter window; the counting rate increasing as the anode was extended towards the window. Apparently, many electrons entering the counter at the large angle relative to the axis do not get back into the sensitive region behind the anode tip. Lower energy particles will be more effectively scattered back off the counter wall into the sensitive region. The remaining deviation from linearity of the Kurie plot was removed by inserting the scattering baffle and lining the walls of the spectrometer chamber with 1/16 inch magnesium. The resulting Kurie plot is shown in Fig. 18c. A straight Kurie plot was also obtained for Y^{91} from the maximum energy of 1.56 Mev down to 100 kev.

Since there is iron present in the spectrometer, the linearity of the current-momentum relationship is uncertain. To check this and to determine the equation by which the momentum of focused electrons may be calculated, a calibration curve was obtained from known conversion lines. The five conversion lines of Th (B+C+C") were used since they have been accurately determined[12,13,14] by means of 180° spectrometers. These lines give electrons with a fairly wide range in momentum and consequently they are very satisfactory for calibration purposes. These lines give an energy range of 24 kev to 2.5 Mev. The lines are summarized in Table I. Before any data were

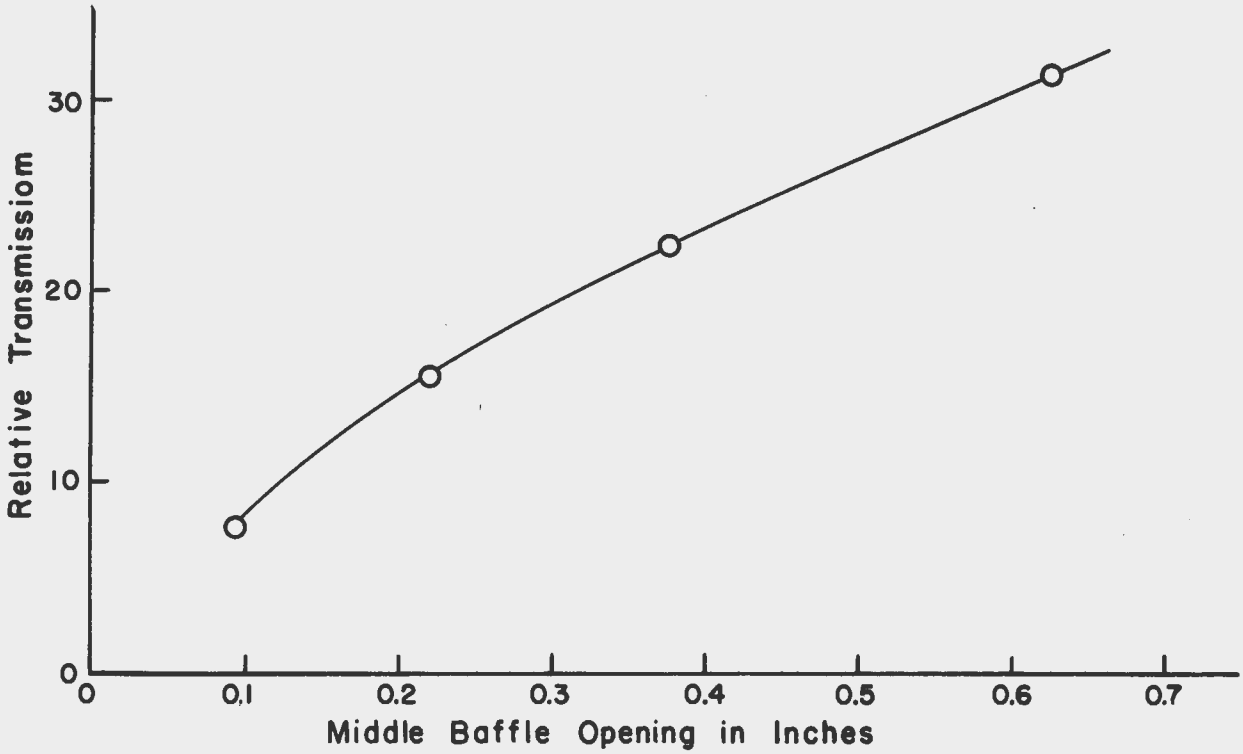

Fig. 15 - Transmission and half-width as a function of defining slit width.

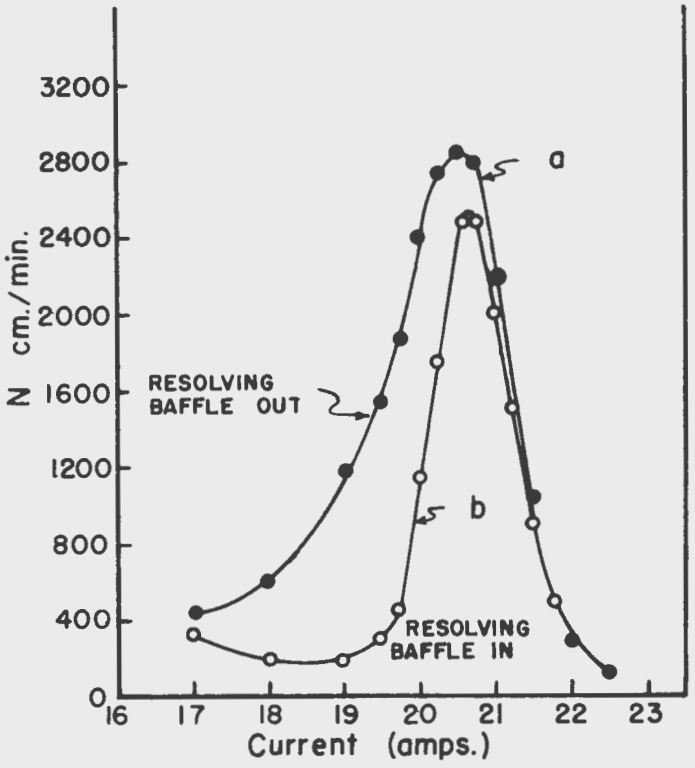

Fig. 16 - Effect of resolving baffle on line spectrum.

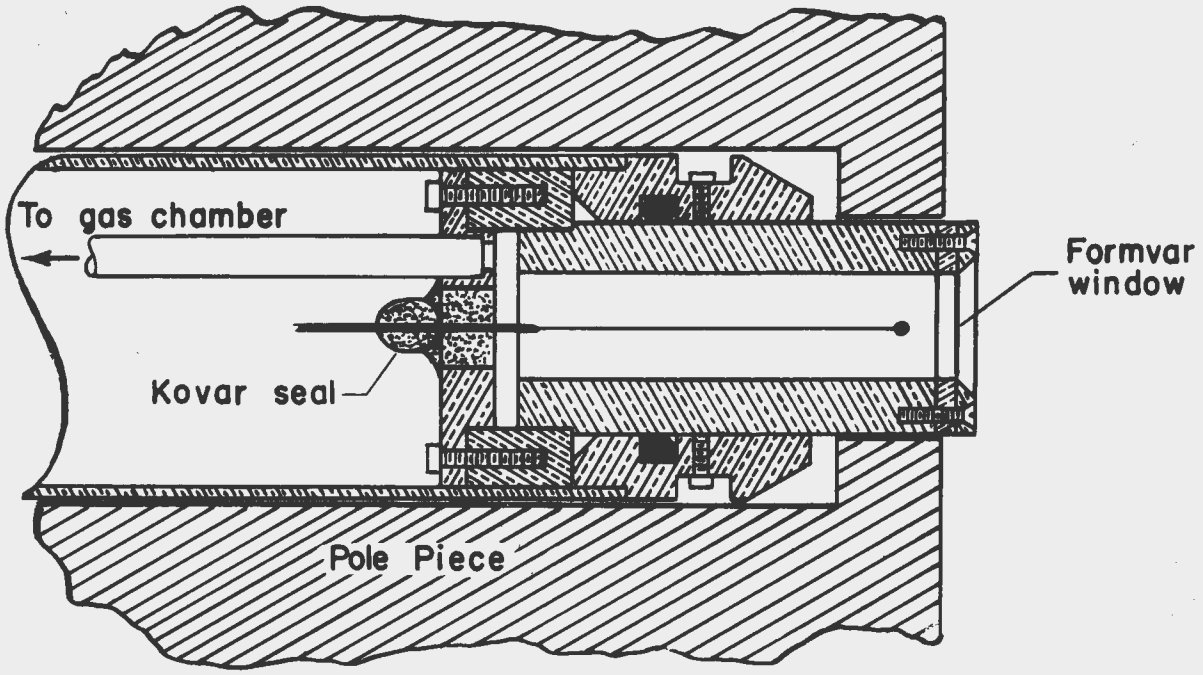

Fig. 17 - Arrangement of Geiger counter used in preliminary adjustments.

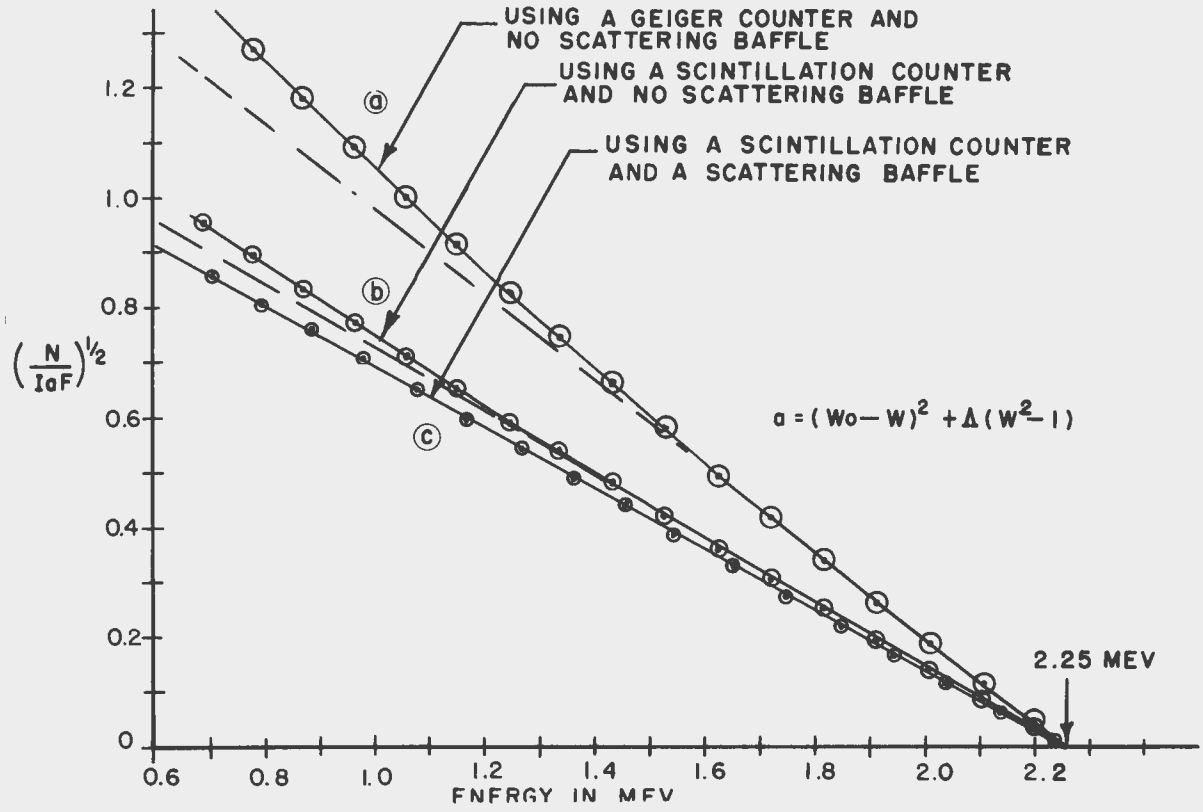

Fig. 18 - Kurie Plots of Y^{90}.

Table I

Thorium Calibration Lines

Source	Line	Momentum in $H\rho$	Reference
Th B	F	1,388.55±0.20	12
Th B	I	1,754.01±0.25	12
Th C	A	533.66±0.12	13
Th C"	L	2,607.18±0.35	12
Th C"	X	9,988.4 ±2.0	14

taken, the current in the spectrometer was increased to a hundred amp which is the maximum operating current. It was then decreased to zero. By always repeating this procedure before taking data and by taking data for successively increasing values of current, the effect of residual magnetism was kept constant. Using this procedure, the conversion lines of Th(B+C+C") were examined and the results are indicated in Fig. 19. Within experimental error, the relation between current and momentum is linear in this range. The least squares line was determined. The equation for normal operation with the 5/8 inch defining baffle is given by

$$H\rho = 165.1\ (I+0.033),$$

where $H\rho$ is the momentum of the focused electrons in gauss-cm and I is the current in the spectrometer coils in amp. The constant added to the current represents a displacement of the calibration line to the left of the origin and is due to residual magnetism. An indication of the current-momentum relation at higher currents has been obtained from measurement of the high energy beta-ray in Rh^{106}. The resulting value for the maximum energy was 3.56±0.03 Mev compared to Alburger's[15] value of 3.53±0.01 Mev, which was obtained with an iron-free thin-lens spectrometer.

The first step in using the coincidence spectrometer is the determination of the resolving time of the coincidence circuit. The effective resolving time is calculated from the equation

$$N_a = 2N_b N_g T,$$

where N_a is the accidental coincidence rate, N_b and N_g are the beta and gamma counting rates, respectively, and T is the effective resolving time. The resolving time is found experimetally by using

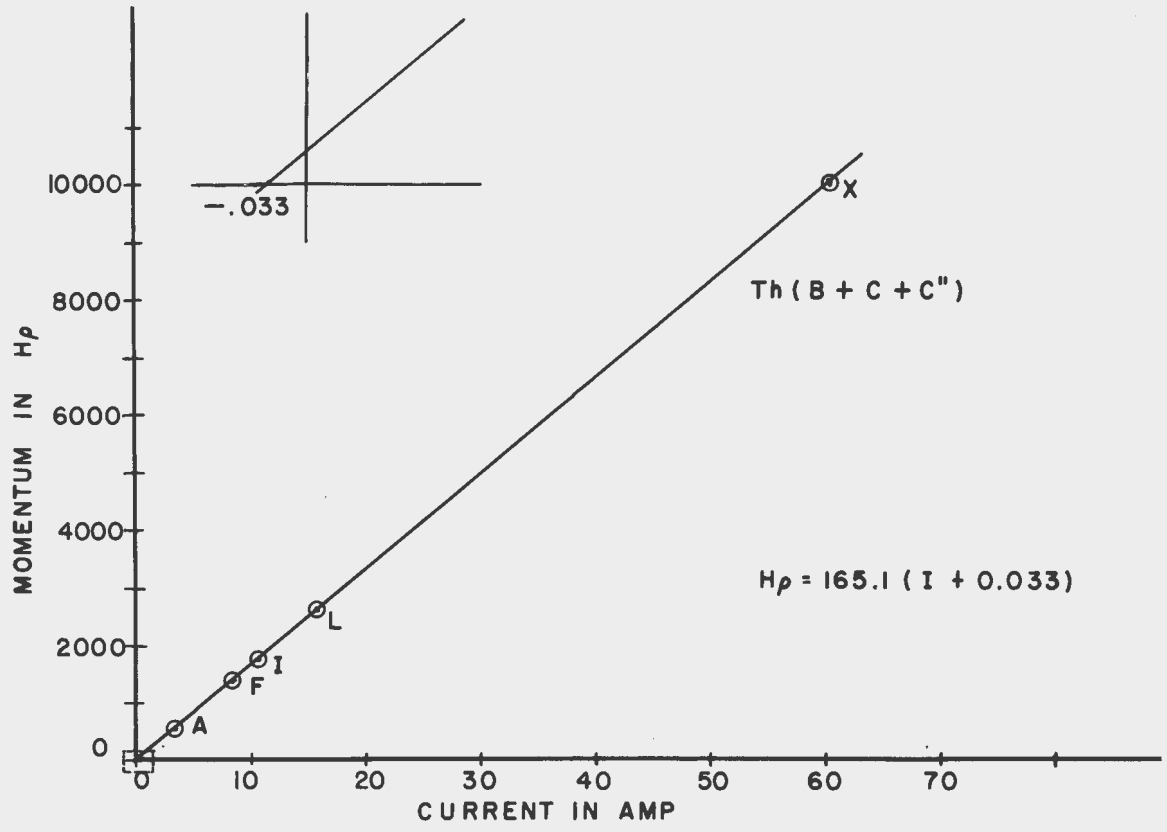

Fig. 19 - Calibration curve of spectrometer from conversion lines in Th(B+C+C'').

separate sources in the beta-ray spectrometer and the gamma-ray spectrometer. Besides the previously mentioned influence of pulse time variation on the resolving time, there may be another effect which is also energy dependent. If either the beta-scaler or coincidence circuit are sensitive to beta signals which are not large enough to operate the other, there will be a change in effective resolving time at low beta-energy settings. However, this effect will be accounted for by the experimental determination of resolving times for various energies. The resolving time of the coincidence apparatus is about 0.8 microsecond at high beta energies and diminishes as the energy is decreased.

The next step in calibrating the instrument was to check the operation of the coincidence spectrometer by use of a known coincidence transition. For this purpose, a Au^{198} source was used. The decay scheme of Au^{198}, which is shown in Fig. 20, consists almost entirely of a single beta-group, having an allowed shape, which is in coincidence with a gamma-ray.[16] Because all gamma-rays are in coincidence with beta-particles and about 99% are of the same energy, the coincidence spectrum should agree almost exactly with the beta-spectrum. Any discrepancy between the two spectra can be detected by direct comparison. The two spectra agreed. Both the total beta-spectrum and the coincidence spectrum had the same end-point energy of 967±5 kev and the ratio of coincidence to total counts was constant within statistical error for all experimental points. The spectra of Au^{198} are shown in Fig. 20 and the Kurie plots of the spectra are shown in Fig. 21. The source intensity of five microcuries was sufficient to give a peak counting rate of 1100 counts/min for the coincidence beta-spectrum. The deviations at the lower energy ends of the Kurie plots are due to the 1% beta group in Au^{198} and the presence of Au^{199} which is formed by an n,γ reaction with Au^{198} as the Au^{198} is formed in the pile. Au^{199} has a beta end-point energy of 400 kev and the 1% beta-branch in Au^{198} has a maximum energy of 290 kev. A detailed study of the contamination of Au^{198} by Au^{199} was reported by Fan.[17]

The decay scheme of Au^{198} made possible a determination of the transmission of the beta-ray spectrometer under the conditions for which the coincidence spectrum was taken. Let N represent the number of disintegrations per minute, e_B the integrated fraction of the beta-particles which are transmitted and detected (e_B is the effective solid angle of the spectrometer), and e_g the fraction of the gamma-rays which are counted. If there is a beta-particle followed by one gamma-ray for each disintegration, then

$$N_B = Ne_B \text{ and } N_g = Ne_g$$

where N_B is the integrated number of beta-rays counted per minute and N_g is the number of gamma-rays counted per minute. N_B is obtained by integrating over the observed beta-spectrum and dividing by the effective half-width of the transmission function. The probability of a disintegration producing a coincidence count is the product of

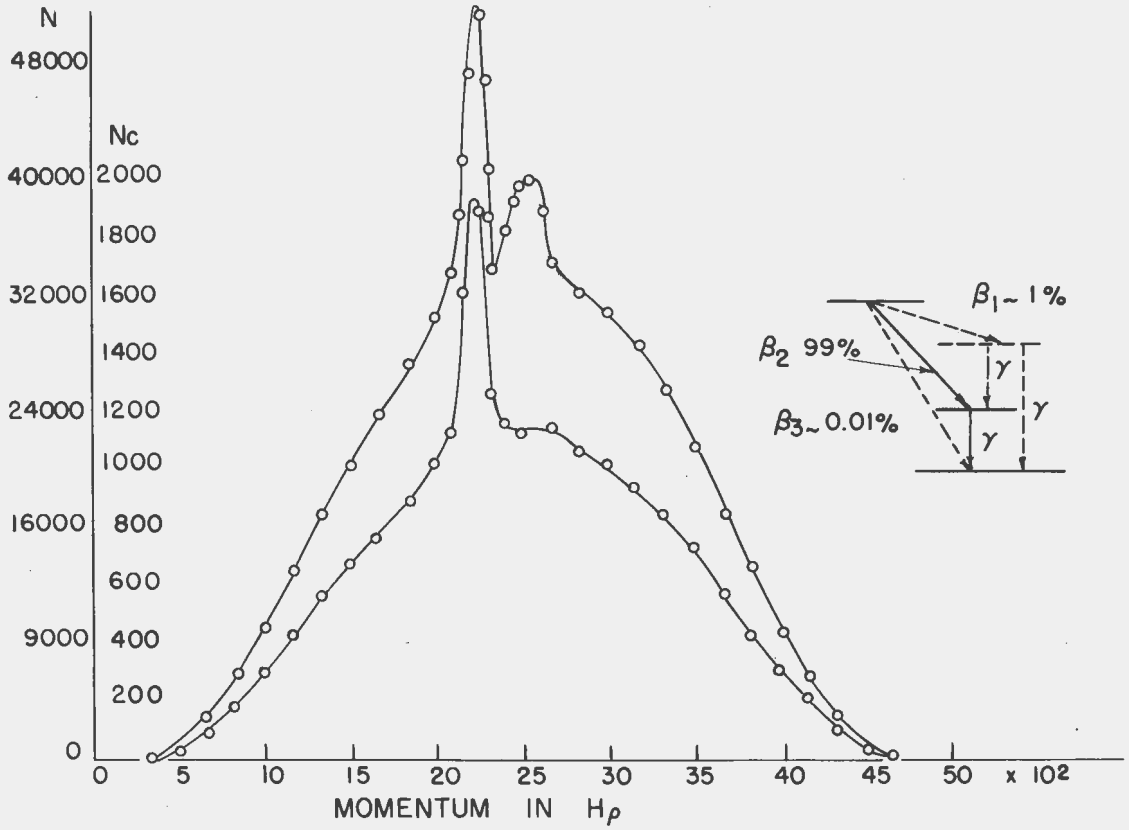

Fig. 20 - Total and coincidence spectra of Au^{198}.

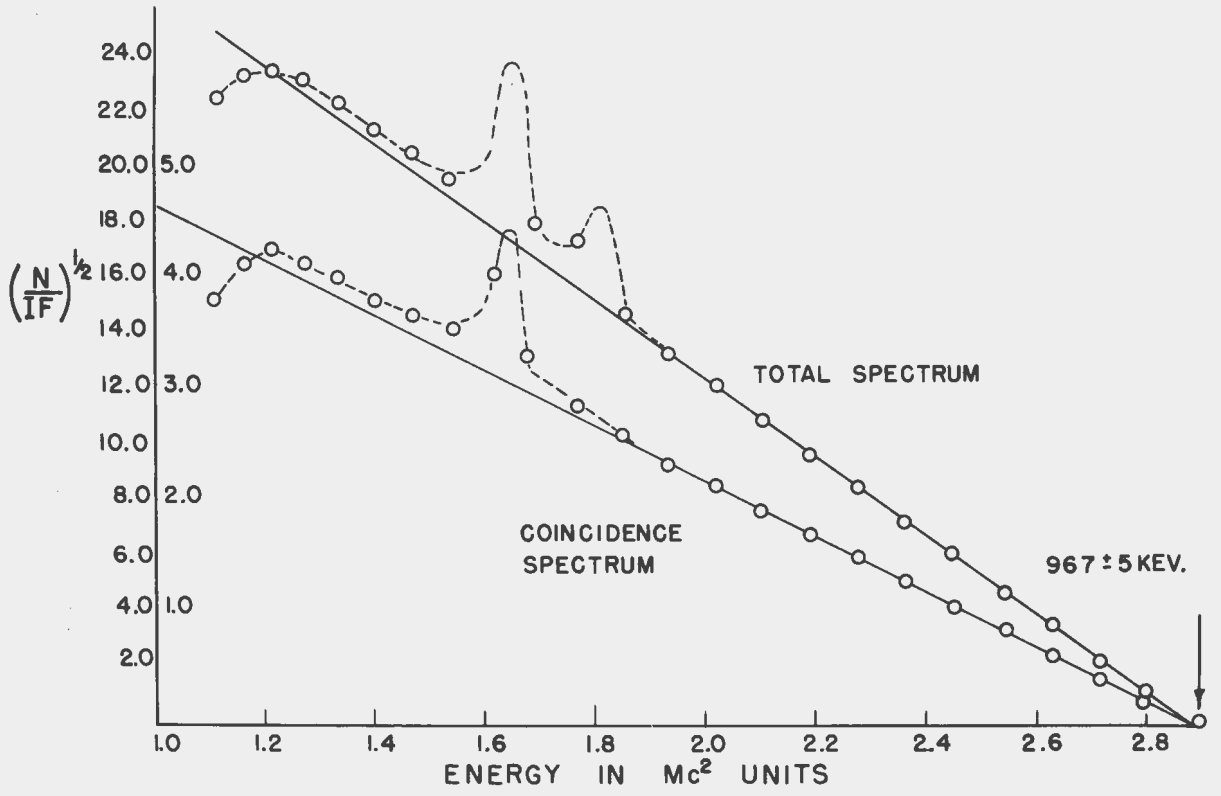

Fig. 21 - Kurie plots of total and coincidence spectra of Au^{198}.

the probability of its producing a beta count and the probability of its producing a gamma count. Thus

$$N_c = Ne_B\, e_g,$$

where N_c is the integral of the observed coincidence spectrum divided by the effective half-width of the transmission function. From N_c and N_g it is possible to determine the solid angle e_B of the spectrometer. Thus

$$\frac{N_c}{N_g} = \frac{Ne_B\, e_g}{N\, e_g} = e_B.$$

Neglecting the other weak beta-groups and considering the Au^{198} decay scheme to consist simply of the 967 kev beta-group followed by the 411 kev gamma-ray, the solid angle of the spectrometer with a 5/8 inch center aperature was obtained from the coincidence data. Using the formula developed above, the solid angle was found to be

$$e_B = \frac{N_c}{N_g} = \frac{33{,}700}{347{,}000} \quad 0.1$$

100 x 0.1 = 10% solid angle.

The gamma-efficiency varies not only with crystal size and position but also with the energy of the gamma-ray. It may be obtained experimentally in a manner similar to the solid angle.

$$\frac{N_c}{N_B} = \frac{Ne_B\, e_g}{Ne_B} = e_g.$$

Because the counting rates of the beta-scaler and the coincidence scaler have this same ratio at all points it is not necessary to integrate to obtain the gamma-efficiency. The gamma-efficiency for the 411 kev gamma-ray in Au^{198} was obtained by averaging the ratios of coincidence counts to beta-counts for a number of points on the spectra above the energy of the gamma-ray. It was found to be 3.2 per cent for this particular gamma energy.

An article describing the work on the beta-spectra of Rb^{86}, Pr^{142}, and Tm^{170} will be submitted to the Phys. Rev.

IV. PROPOSED CHANGES

A research instrument may not be expected to remain static in form. Frequent modification is necessary to improve it and to extend its application. A few contemplated changes should be mentioned here.

A defining baffle with a continuously variable aperature width is now under construction. It is a modification of a drawing kindly supplied by K. Siegbahn and H. Slätis. The aperature in this baffle may be set to any width up to one inch by means of a control which is outside of the spectrometer.

A helical type charge-discriminating baffle is to be constructed for distinguishing electron and positron radiation. It is to be inserted or removed from the transmitted beam by external controls.

An increase in the efficiency of the gamma-detector is to be accomplished by enlarging the opening in the pole piece and increasing the size of the scintillation crystal.

V. ACKNOWLEDGMENTS

The authors wish to express their appreciation to J. D. Clement, presently in the United States Armed Forces, for his part in the planning and construction of this instrument. Thanks are also due to Mr. A. A. Read and his associates in the Electronics Shop for the design and construction of the current control, to Mr. I. O. Coleman of the College Instrument Shop and his staff for production of many parts of this spectrometer and to Wayne Rhinehart for many useful suggestions for improving the detecting equipment, and the design of the linear amplifiers.

VI. LITERATURE CITED

1. H. Slätis and K. Siegbahn, Arkiv. f. Fysik 1, 339 (1949).
2. E. N. Jensen, L. J. Laslett, and W. W. Pratt, Phys. Rev. 75, 458 (1949).
3. W. W. Pratt, F. I. Boley, and R. T. Nichols, Rev. Sci. Instr. 22, 92 (1951).
4. W. Glaser, Zeit. f. Physik 116, 19 (1940).
5. K. Siegbahn, Phil. Mag. 37, 169 (1946).
6. H. O. Richardson, Phil. Mag. 40, 233 (1949).
7. W. Bothe, Naturwiss. 37, 41 (1950).
8. J. Fischer and J. Marshall, Rev. Sci. Instr. 23, 417 (1952).
9. J. E. Francis, Jr., P. R. Bell, and J. C. Gundlach, Rev. Sci. Instr. 22, 133 (1951).
10. J. P. Palmer, Doctorate Thesis (Iowa State College, 1950).
11. E. N. Jensen and L. J. Laslett, Phys. Rev. 75, 1949 (1949).
12. G. Lindstrom, Phys. Rev. 83, 465 (1951).
13. H. Craig, Phys. Rev. 85, 688 (1952).
14. W. L. Brown, Phys. Rev. 83, 271 (1951).
15. D. E. Alburger, Phys. Rev. 88, 339 (1952).
16. Hollander, Perlman, and Seaborg, Univ. of Calif. Rad. Lab. Report-1928 (Berkeley, 1952).
17. Chang-Yun Fan, Phys. Rev. 87, 252 (1952).